Self-phase-modulation near electronic resonances of a crystal*

R. R. Alfano, J. I. Gersten, and G. A. Zawadzkas
Department of Physics, City College of the City University of New York, New York, New York 10031

N. Tzoar†
Department of Physics, Bar-Ilan University, Ramat Aviv, Israel
(Received 7 January 1974)

Frequency broadening generated by picosecond laser pulses is investigated experimentally and theoretically near the electronic levels of a PrF_3 crystal. Information is obtained on the role played by the electronic levels on self-phase-modulation and four-photon parametric emission, and on how the self-phase-modulation spectrum evolves through and beyond the electronic absorption levels.

I. INTRODUCTION

When a sufficiently intense light pulse propagates through a material, it distorts the atomic configuration, which in turn causes the refractive index to acquire a time dependence. The mechanisms which can contribute to this refractive index change[1] for an ultrashort pulse are direct distortion of electronic clouds,[2] librational motion of molecules or atomic clusters,[3] molecular orientation[4] or redistribution,[5] or a coupled mechanism. The time-varying index alters the phase of the optical wave as it propagates, leading in general to a broadening of the pulse spectrum. The process has been called self-phase-modulation (SPM) or superbroadening.[6] Spectral broadening was first observed in CS_2 by Brewer[7] and interpreted in terms of SPM by Shimizu,[8] who attributed the broadening to the molecular orientational effect. Libration of the CS_2 molecule has also been proposed to explain these spectra.[9] Brewer and Lee[10] observed self-focusing of picosecond laser pulses in CS_2 and viscous liquids, and suggested that the index nonlinearity is of electronic origin. Alfano and Shapiro[11] using picosecond pulses at 5300 Å observed SPM and self-focusing in various crystals, liquids, and glasses, including liquified and solidified rare gases. They showed that the electronic mechanism for SPM is important in all materials and dominates all other processes in some materials: e.g., liquid argon and krypton. Most recently, Bloembergen[12] proposed an index of refraction charge resulting from avalanche plasma formation as the mechanism for SPM.

Nonlinear effects may play an important role as loss mechanisms in large laser systems. SPM is an example of such a process. Since the active medium of a laser possesses well-defined electronic energy levels, knowledge of SPM near electronic levels is of paramount importance.

Traditionally, SPM has been observed in transparent materials[11,13] and theoretical calculations[14] have neglected both nearby electronic resonances and material dispersion. In this paper SPM near electronic levels of PrF_3 crystal is investigated experimentally and theoretically to gain additional information on the SPM process—in particular, on the role played by the electronic levels and on how the SPM spectrum evolves through and beyond the electronic absorption levels.

II. EXPERIMENT

Experimentally the Stokes and anti-Stokes spectrum and filament formation from PrF_3 crystal is investigated under intense picosecond pulse excitation at the wavelength of 5300 Å. A Nd-glass mode-locked laser[10] generates picosecond light pulses which are converted, in a potassium dihydrogen phosphate (KDP) crystal, to the second harmonic at the wavelength of 5300 Å. The harmonic radiation consists of pulses of about 8×10^8-W power and 4-psec duration. The average energy of a single pulse in a typical train is ~3.2 mJ, as measured with Hadron thermopile. The beam is collimated by an inverted telescope and enters a 5-cm-long PrF_3 crystal with a beam diameter of about 2 mm. The c axis of the crystal is oriented along the optical axis. The intensity distribution at the exit face of the crystal is magnified by 10× and imaged on the 1-mm slit of a Jarrel-Ash $\frac{1}{2}$-m-grating spectrograph, so that the spectrum of each filament is displayed. The spectra are recorded on Polaroid type 57 film. The pulse trains are monitored with ITT photodiode and displayed on Tektronix 519 oscilloscope. The spectra are created by pulse trains whose peak heights vary by no more than 50%. A combination of a 3-mm wire placed at the focal point of the imaging lens and/or Corning filters (Stokes side 3-67, 3-68; anti-Stokes side 5-60, 5-61) is used to prevent any laser light that has not formed filaments from entering the specto-

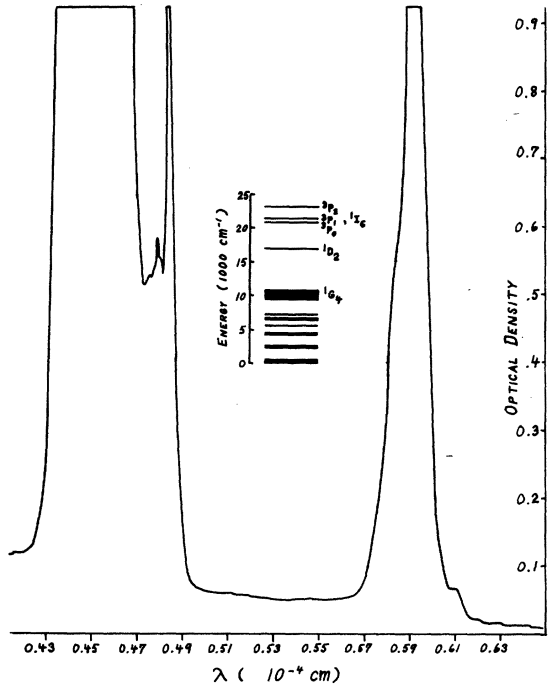

FIG. 1. Absorption spectra of 0.5-mm-thick PrF_3 crystal; insert is the level scheme (Refs. 14 and 15) of Pr^{3+} ions.

graph. A glass beam splitter defects a portion of the beam into a camera where the filaments are simultaneously photographed. No visible damage occurred in PrF_3 crystal.

The PrF_3 crystal is chosen for the experiment because its electronic levels are suitably located on the Stokes and anti-Stokes sides of the 5300-Å excitation wavelength. The absorption spectra of $\frac{1}{2}$-mm-thick PrF_3 crystal and the energy-level scheme of Pr^{3+} ions[15] are shown in Fig. 1. The fluorides of Pr have a structure of the naturally occurring mineral tysonite with a D_{3d}^4 symmetry.[16]

Typical spectra showing frequency broadening from PrF_3 about 5300 Å are shown in Fig. 2 for different laser shots. Because of the absorption associated with the electronic levels it is necessary to display the spectrum over different wavelength ranges at different intensity levels. In this manner, the development of the SPM spectrum through the electronic absorption levels can be investigated. Using appropriate filters different spectral regions are studied and displayed in the following figures: in Fig. 3(a) the Stokes side for frequency broadening ($\bar{\nu}_B$)>100 cm^{-1} at intensity level (I_{SPM}) of ~10^{-2} of the laser intensity (I_L); in Fig. 3(b) the Stokes side for $\bar{\nu}_B$>1500 cm^{-1} at I_{SPM} ~$10^{-4} I_L$; in Fig. 3(c) the anti-Stokes side for $\bar{\nu}_B$>100 cm^{-1} at I_{SPM} ~$10^{-2} I_L$; and in Fig. 3(d) the anti-Stokes side for $\bar{\nu}_B$>1500 cm^{-1} at I_{SPM} ~$10^{-4} I_L$. Usually 50–100 small-scale filaments 5–50 μm in diam are observed.

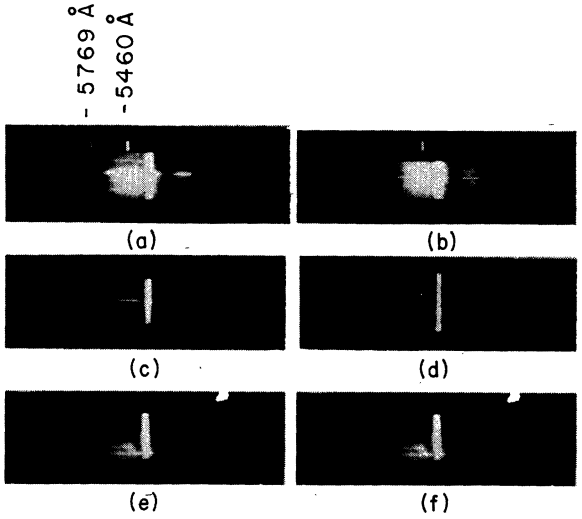

FIG. 2. Frequency broadening from PrF_3 about the 5300-Å psec laser excitation; neutral density (ND) filters: (a) ND=1.5; (b) ND=1.5; (c) ND=2.0; (d) ND =2.0; (e) ND=1.7, (f) ND=1.4. A wire is positioned after the collection lens at the focal length.

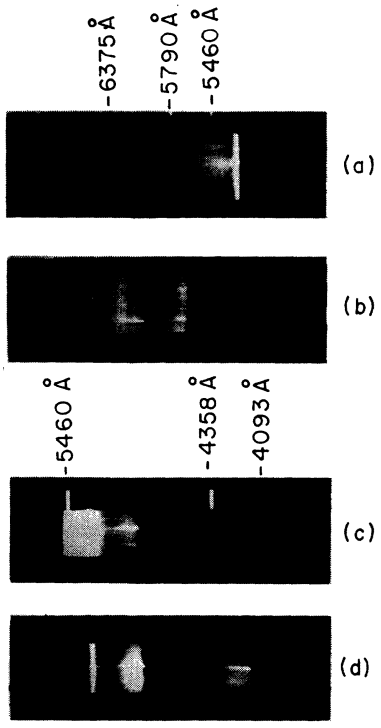

FIG. 3. Frequency broadening on the Stokes and anti-Stokes side of the 5300-Å excitation. (a) Stokes side, Corning 3-68 filter, wire inserted, ND=2.0; (b) Stokes side, Corning 3-66 filter, wire inserted; (c) anti-Stokes side, wire inserted, ND=1.0; (d) anti-Stokes side, Corning 5-61 filter, wire inserted.

Several salient features are evident in the spectra displayed in Figs. 2 and 3. In Fig. 2 the Stokes and anti-Stokes spectra are approximately equal in intensity and frequency extent. The peak intensity at the central frequency is $\sim 10^2$ the intensity of the SPM at a given frequency. The extent of the frequency broadening is ~1500 cm^{-1}, ending approximately at the absorption lines. Occasionally a periodic structure of minima and maxima is observed which ranges from a few cm^{-1} to 100 cm^{-1}, and for some observations no modulation is observed. Occasionally an absorption band appears on the anti-Stokes side of the 5300-Å line whose displacement is 430 cm^{-1} and whose width is 400 cm^{-1}. In Fig. 3 the main feature is the presence of a much weaker super-broadband continuum[11] whose frequency extends through and past the well-defined absorption lines of the Pr^{3+} ion to a maximum frequency of >3000 cm^{-1} on the stokes side (end of film sensitivity) and >6000 cm^{-1} on the anti-Stokes side. The intensity of the continuum at a given frequency outside the absorption lines is $\sim 10^{-4}$ the laser intensity.

The observed absorption lines on the anti-Stokes side of 5300 Å are located at 4415, 4653, and 4845 Å and on the Stokes side at 5930 and 6109 Å. These lines correspond within ±7 Å to the absorption lines measured with a Cary 14. The absorption coefficients measured from the Cary spectra are ~3 cm^{-1} at 6112 Å, 62 cm^{-1} at 5938 Å, 46 cm^{-1} at 4852 Å, and >100 cm^{-1} at 4412 and 4647 Å.

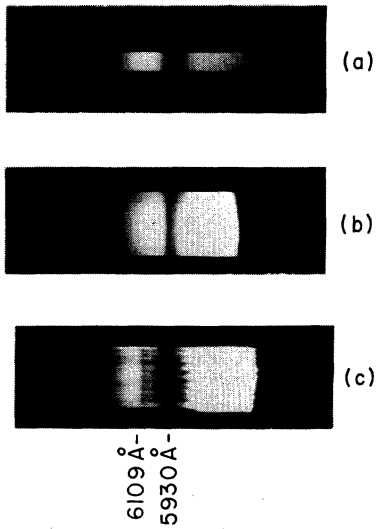

FIG. 4. Comparison of the Stokes absorption spectra of PrF_3 photograph with different light sources: (a) light emitted from a tungsten lamp is passed through 0.5-mm-thick PrF_3 crystal; (b) SPM light emitted from BK-7 is passed through 0.5-mm-thick crystal; (c) SPM light is generated within the 5-cm PrF_3.

Figure 4 compares the Stokes absorption spectra of PrF_3 crystal photographed with $\frac{1}{2}$-m Jarrel Ash spectrograph with different broadband light sources. Figure 4(a) is obtained with light emitted from a tungsten lamp passing through $\frac{1}{2}$-mm PrF_3 crystal; Fig. 4(b) is obtained with the Stokes side of the broadband picosecond continuum generated in BK-7 glass passing through $\frac{1}{2}$-m PrF_3; and Fig. 4(c) is obtained with the broadband light generated in 5-cm PrF_3 crystal. Notice that the absorption line at 6112 Å is very pronounced in the spectra obtained with the continuum generated in PrF_3, while with conventional absorption techniques it is just barely visible. The anti-Stokes spectrum obtained from light emitted from a tungsten filament lamp passing through $\frac{1}{2}$-mm PrF_3 crystal is given in Fig. 5(a). This is to be compared with the spectrum obtained with broadband light generated in a 5-cm PrF_3 crystal given in Fig. 5(b).

The angular variation of the anti-Stokes and Stokes spectral emission emitted from PrF_3 is displayed in Fig. 6. The light emitted from the sample is focused on the slit of $\frac{1}{2}$-m Jarrel Ash spectrograph with 5-cm focal length lens with the laser beam positioned near the bottom of the slit so that only the upper half of the angular spectrum curve is displayed. In this fashion a larger angular variation of the spectrum is displayed. Emission angles >9° go off slit and are not displayed. This spectrum is similar to four-photon emission patterns observed from glass and liquids[11] under picosecond excitation.

III. THEORY

A. Basic equations of self-phase-modulation

The one-dimensional propagation of linearly polarized light in an absorptive and nonlinear medium will be studied in this paper. Letting E denote the electric field strength, D the electric

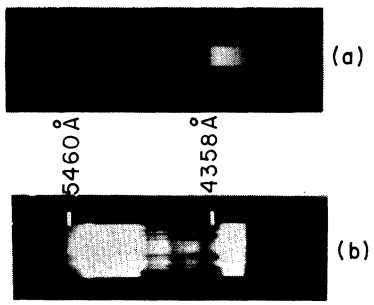

FIG. 5. Comparison of the anti-Stokes absorption spectrum of PrF_3 photograph with (a) light emitted from a tungsten lamp passing through 0.5-mm-thick crystal; (b) SPM light generated within the 5-cm PrF_3.

displacement, and z the propagation direction, the wave equation is written as

$$\frac{\partial^2 E}{\partial z^2} - \frac{\partial^2 D}{\partial t^2} = 0. \tag{1}$$

It will be assumed that both E and D are describable by a slowly varying amplitude and phase. Let ω denote the radian frequency and $k = \omega(\epsilon_0)^{1/2}/c$ denote the propagation constant, where $v = c/(\epsilon_0)^{1/2}$ is the speed of light of a weak signal in the medium. Then

$$E = \mathcal{E}\cos(kz - \omega t + \varphi), \tag{2a}$$

$$D = \mathfrak{D}_1 \cos(kz - \omega t + \varphi) + \mathfrak{D}_2 \sin(kz - \omega t + \varphi), \tag{2b}$$

where $\mathcal{E}$, $\mathfrak{D}_1$, $\mathfrak{D}_2$, and φ are dependent on z and t. If one inserts Eqs. (2a) and (2b) into Eq. (1) and neglects second-order derivatives and squares of first-order derivatives as being small, one obtains the set

$$-2kc^2 \frac{\partial \mathcal{E}}{\partial z} = 2\omega \frac{\partial \mathfrak{D}_1}{\partial t} - \omega^2 \mathfrak{D}_2 + 2\omega \mathfrak{D}_2 \frac{\partial \varphi}{\partial t}, \tag{3}$$

$$-2kc^2 \frac{\partial \varphi}{\partial z}\mathcal{E} = k^2 c^2 \mathcal{E} - \omega^2 \mathfrak{D}_1 + 2\omega \mathfrak{D}_1 \frac{\partial \varphi}{\partial t} - 2\omega \frac{\partial \mathfrak{D}_2}{\partial t}. \tag{4}$$

The nonlinearity to be considered in this paper is the one generated by the common dielectric function of the form $\epsilon_0 + \epsilon_2 E^2$. The absorption is due to a resonant line at frequency ω_a and is described as a response transform of the electric field. Thus the electric displacement is given by

$$D = \epsilon_0 E + \epsilon_2 E^3 - 2f \int_{-\infty}^{0} d\tau\, E(t+\tau) e^{\gamma\tau/2} \sin\omega_a \tau, \tag{5}$$

where γ is the decay rate for the excited state of the medium and f measures the strength of the absorption. In this section we restrict our attention to the case of a single absorption line, although the extension to the multiline case is trivial. One notices that the solution of Eq. (1) is complicated by the fact that D is both a nonlinear and nonlocal (in time) function of E.

A further complication arises from the fact that the term $\epsilon_2 E^3$ contains an admixture of the third harmonic of ω. While this term is of importance in analyzing third-harmonic generation, since we are concerned in this paper with the neighborhood of ω we ignore the 3ω contribution. Thus we write

$$E^3 = \tfrac{1}{4}\mathcal{E}^3\{3\cos(kz - \omega t + \varphi) + \cos[3(kz - \omega t + \varphi)]\}, \tag{6}$$

and simply drop the second term.

The absorptive term of Eq. (5) may be simplified somewhat by making several approximations. In the expansion of the product $E(t+\tau)\sin\omega_a\tau$ there appear resonant terms involving $\omega - \omega_a$ and nonresonant terms involving $\omega + \omega_a$. The latter terms will be highly oscillatory and hence not contribute appreciably to the absorption, so only the resonant terms will be kept. A second approximation is based on the fact that we will be mainly concerned with pulse propagation through the medium. Thus $\mathcal{E}$ will be fairly sharply peaked in time and the phase in the immediate vicinity of the pulse is all that need enter the formalism. This allows us to replace $\varphi(t+\tau)$ by an appropriately truncated power series: $\varphi(t+\tau) \approx \varphi(t) + \tau\dot{\varphi}(t)$. A fuller discussion is presented in Appendix A. Combining Eqs. (2) and (5) we then find

$$\mathfrak{D}_1 = \epsilon_0 \mathcal{E} + \frac{3}{4}\epsilon_2 \mathcal{E}^3 + \frac{f\mathcal{E}[\omega_a - \omega + (\partial\varphi/\partial t)]}{(\gamma/2)^2 + [\omega_a - \omega + (\partial\varphi/\partial t)]^2}, \tag{7a}$$

$$\mathfrak{D}_2 = -\frac{f\mathcal{E}(\gamma/2)}{(\gamma/2)^2 + [\omega_a - \omega + (\partial\varphi/\partial t)]^2}. \tag{7b}$$

Insertion of Eqs. (7a) and (7b) into Eqs. (3) and (4) leads to rather complex equations, so further approximations are warranted. It will be assumed that the nonlinearity is sufficiently weak that products of nonlinear terms with slowly varying terms may be dropped. Indeed the assumption of a small ϵ_2 term is consistent with writing the dielectric function in the form $\epsilon_0 + \epsilon_2\mathcal{E}^2 + \cdots$. In addition it will be assumed that the absorption is mild enough so that products of absorptive terms with slowly varying terms may also be neglected. Finally, dispersive effects will be disregarded as they are generally weak. Thus we find the following set of

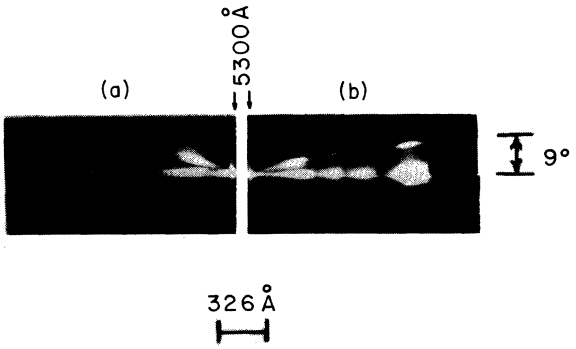

FIG. 6. Angular variation of the (a) Stokes and (b) anti-Stokes spectral patterns emitted from PrF_3 crystal: (a) Corning 4-(3-67) filters, ND = 1.0; (b) Corning 2-(5-60) filters.

equations for the amplitude and phase:

$$\frac{\partial \mathcal{E}}{\partial t} + v\frac{\partial \mathcal{E}}{\partial z} = -\frac{\pi\omega f}{2\epsilon_0}\mathcal{E}\Delta\left(\omega_a - \omega + \frac{\partial\varphi}{\partial t}\right), \tag{8}$$

$$\frac{\partial \varphi}{\partial t} + v\frac{\partial \varphi}{\partial z} = \frac{3}{8}\frac{\omega\epsilon_2}{\epsilon_0}\mathcal{E}^2, \tag{9}$$

where Δ is the Lorentzian function

$$\Delta(x) = \frac{1}{\pi}\frac{\gamma/2}{(\gamma/2)^2 + x^2}. \tag{10}$$

As discussed in Appendix A, Eq. (10) refers to the case where the radiative lifetime is shorter than the pulse duration. In the other extreme, where it is longer, we replace Eq. (10) by the Gaussian representation

$$\Delta(x) = \frac{1}{2\pi}\left(\frac{\pi}{\lambda}\right)^{1/2} e^{-x^2/4\lambda},$$

where $\lambda = 1/D^2$ and D is the duration of the pulse.

Equations (8) and (9) form the basic equations governing the self-phase-modulation of light in a nonlinear absorptive medium. A solution to these equations will be sought in the subsequent sections.

B. Solution to self-phase-modulation equations

Before an explicit solution can be found, the boundary conditions must be specified. In typical experimental situations one has the pulse injected into the medium at some boundary, which will be taken as the point $z = 0$. Thus we assume

$$\mathcal{E}(0, t) = H(t) \tag{11}$$

and

$$\varphi(0, t) = 0, \tag{12}$$

where the function $H(t)$ is usually sharply peaked around $t = 0$.

It is profitable to rewrite the basic equations of self-phase-modulation as a single second-order nonlinear parabolic equation. Let us introduce two new independent variables,

$$\xi = t - (z/v) \tag{13a}$$

and

$$\eta = t + (z/v). \tag{13b}$$

Then Eqs. (8) and (9) may be combined to give

$$\frac{\partial^2\varphi}{\partial\eta^2} = -\alpha\frac{\partial\varphi}{\partial\eta}\Delta\left(\Omega + \frac{\partial\varphi}{\partial\xi} + \frac{\partial\varphi}{\partial\eta}\right), \tag{14}$$

where the following definitions have been made for economy of notation:

$$\Omega = \omega_a - \omega \tag{15}$$

and

$$\alpha = \pi\omega f/2\epsilon_0. \tag{16}$$

Also, let

$$\beta = \tfrac{3}{16}(\omega\epsilon_2/\epsilon_0), \tag{17}$$

and

$$I(t) = H^2(t), \tag{18}$$

so the boundary conditions may be written as

$$\left.\frac{\partial\varphi}{\partial\eta}\right|_{\xi=\eta} = \beta I(\xi), \tag{19}$$

and

$$\varphi|_{\xi=\eta} = 0. \tag{20}$$

The range of interest is the domain $\eta \geq \xi$.

Before undertaking the general solution of Eq. (14) let us first examine the nonabsorptive limit ($\alpha = 0$) of the equation. The solution which satisfies Eqs. (19) and (20) is

$$\varphi(\xi, \eta) = \beta I(\xi)(\eta - \xi). \tag{21}$$

From Eq. (2a) it is apparent that the instantaneous frequency of the wave is

$$\omega(t) = \omega - \frac{\partial\varphi}{\partial t} = \omega - \frac{\partial\varphi}{\partial\xi} - \frac{\partial\varphi}{\partial\eta}. \tag{22}$$

From Eq. (21) we therefore find

$$\omega(t) = \omega - (2\beta z/v)I'[t - (z/v)]. \tag{23}$$

This gives rise to the customary sweep of frequencies observed in self-phase-modulation experiments.

Now we return our attention to the more general case where absorption is present. It will be assumed that the spectral decay rate γ is sufficiently small that Δ may be considered, for all intents and purposes, a Dirac δ function. In such a case it is clear that Eq. (21) represents a solution to Eq. (14) in a fair portion of the $\xi - \eta$ plane. The resonance region, where

$$\Omega + \frac{\partial\varphi}{\partial\xi} + \frac{\partial\varphi}{\partial\eta} = 0, \tag{24}$$

obviously requires special attention. Physically this condition gives the condition for resonance between the instantaneous frequency $\omega(t)$ and the absorption line frequency ω_a. The argument of the δ function passes through zero at this point and absorptive effects are very important. Insertion of Eq. (21) into Eq. (24) results in an expression for the resonance frontier:

$$\eta = B(\xi) \equiv \xi - [\Omega/\beta I'(\xi)]. \tag{25}$$

As an aid to visualizing the form of the above resonance curve consider a particular form for $H(t)$. Let

$$H(t) = \mathcal{E}_0\,\mathrm{sech}(t/\tau), \tag{26}$$

where $\mathcal{E}_0$ is the peak electric field of the input pulse and τ is a measure of the pulse duration. Expressed in the $z-t$ coordinate system the solution to Eq. (25) is

$$\frac{z}{z_0}=\frac{\cosh^3\{(1/\tau)[t-(z/v)]\}}{\sinh\{(1/\tau)[t-(z/v)]\}}, \tag{27}$$

where

$$z_0=\frac{\Omega v\tau}{4\beta\mathcal{E}_0^2}. \tag{28}$$

For values of z less than $|z_0|$ there is no real solution to Eq. (27) so absorptive effects are completely absent. In order to understand the significance of this statement we return to Eq. (23). It is observed that the frequency sweep has a term proportional to z. For small z the sweep is small and it is possible that $\omega(t)$ will not be equal to ω_a for any value of t. Thus absorption is not important until the point $z=z_0$, where the resonance occurs. In Fig. 7 we present a schematic presentation of the boundary curve for the two cases $\omega-\omega_a>0$ and $\omega-\omega_a<0$. Here we assume that $\epsilon_2>0$, although this restriction may be lifted without much difficulty. In the remainder of this section we will return to the general expression for the boundary conditions involving $H(t)$ or $I(t)$.

Beyond the resonance curve the argument of the δ function again vanishes so the general solution to Eq. (14) may be written as

$$\varphi(\xi,\eta)=F(\xi)+\eta G(\xi), \tag{29}$$

where $F(\xi)$ and $G(\xi)$ are so far arbitrary. However, the definition of the resonance curve must agree when approached from either side, so combining Eq. (29) with Eq. (24) yields

$$\Omega+F'(\xi)+B(\xi)G'(\xi)+G(\xi)=0. \tag{30}$$

Let us now express the argument of the δ function as

$$\Omega+\frac{\partial\varphi}{\partial\xi}+\frac{\partial\varphi}{\partial\eta}=\beta I'(\xi)[\eta-B(\xi)]\Theta(B(\xi)-\eta)+G'(\xi)[\eta-B(\xi)]\Theta(\eta-B(\xi)), \tag{31}$$

where $\Theta(x)=+1$ for positive x and zero for negative x. The argument of the δ function is discontinuous but may be handled through the relation

$$\delta(ax\Theta(x)+bx\Theta(-x))=\frac{1}{2}\left(\frac{1}{|a|}+\frac{1}{|b|}\right)\delta(x). \tag{32}$$

This relation is readily proven by employing $\Delta(x)$ of Eq. (10) and taking the limit $\gamma\to 0$.

Consequently Eq. (14) reduces to

$$\frac{\partial}{\partial\eta}\left(\ln\frac{\partial\varphi}{\partial\eta}\right)=-\frac{\alpha}{2}\left(\frac{1}{|\beta I'(\xi)|}+\frac{1}{|G'(\xi)|}\right)\delta(\eta-B(\xi)). \tag{33}$$

Integration across the resonance curve results in

$$\left(\frac{\partial\varphi}{\partial\eta}\right)_+=\left(\frac{\partial\varphi}{\partial\eta}\right)_-\exp\left[-\frac{\alpha}{2}\left(\frac{1}{|\beta I'|}+\frac{1}{|G'|}\right)\right], \tag{34}$$

where the minus sign denotes the preresonance region and the plus sign denotes the postresonance region. Combining Eq. (34) with Eqs. (21) and (29) yields

$$G(\xi)=\beta I(\xi)\exp\left[-\frac{\alpha}{2}\left(\frac{1}{|\beta I'|}+\frac{1}{|G'|}\right)\right]. \tag{35}$$

Equations (30) and (35) are differential equations for the two unknown functions $G(\xi)$ and $F(\xi)$.

It is reassuring to observe that in the limit of $\alpha\to 0$, where the strength of the absorption may be neglected, we have $G(\xi)=\beta I(\xi)$. Insertion of this into Eq. (30) then gives, upon integration, $F(\xi)=-\beta\xi I(\xi)$, so Eq. (29) reduces to Eq. (21). Thus the resonance curve has little influence when the coupling to the system is small, as should be expected.

The argument of the exponent of Eq. (35) is positive, so for nonzero values of α, $G(\xi)$ is less than $\beta I(\xi)$. This is interpreted as the attenuation effect of the absorption by the system.

Let us first examine the solution to Eq. (35) in the weak-coupling case (small α). We insert the $\alpha=0$ solution for $G'(\xi)$ into the right-hand side to

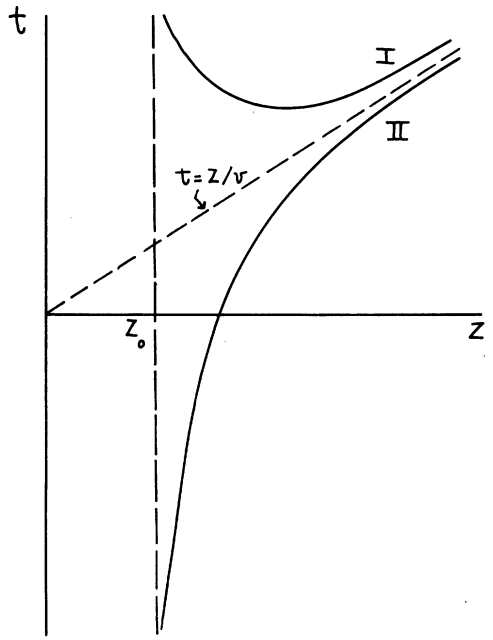

FIG. 7. Resonance curve of Eq. (25) for two cases. Case 1 is for $\omega>\omega_\alpha$ while case 2 is for $\omega<\omega_\alpha$.

obtain a first approximation:

$$G(\xi)\approx\beta I(\xi)\exp\left(\frac{-\alpha}{|\beta I'|}\right). \tag{36}$$

One may obtain an exact validity criterion for this approximation by simply demanding $\alpha\ll|\beta I'(\xi)|$. Thus the discontinuity is weak.

In the strong-absorption limit (large α) the attenuation is rather severe, so $G(\xi)$ will be small. As a first approximation we can simply take

$$G(\xi)\approx 0. \tag{37}$$

The efficacy of this approximation is shown by noting that $-\alpha/|G'(\xi)|$ is then extremely large and negative, so the right-hand side of Eq. (35) is extremely small. Integration of Eq. (30) then gives

$$F(\xi)\approx-\Omega\xi. \tag{38}$$

It does not appear possible to find an analytic solution to Eqs. (30) and (35) in the general case (arbitrary I and arbitrary α). We do not attempt to integrate these equations numerically in this paper.

IV. FOURIER ANALYSIS OF PULSE

The most readily accessible experimental probe of the pulse propagation is the Fourier spectrum of the intensity as a function of Z. Let σ denote the frequency of observation. Then we are interested in finding the spectral function

$$S(Z,\sigma)=\left|\int_{-\infty}^{\infty}dt\,e^{i\sigma t}\,\mathcal{E}(z,t)\cos(kz-\omega t+\varphi)\right|^2. \tag{39}$$

The Fourier integral is performed by again invoking the slowly varying envelope and phase assumption. Casting aside the nonresonant term, we have

$$S(Z,\sigma)=\frac{1}{4}\left|\int_{-\infty}^{\infty}dt\,e^{i(\sigma t-\omega t+\varphi)}\,\mathcal{E}\right|^2. \tag{40}$$

The method of stationary phase is employed in evaluating the integral. Let t_0 be the time at which resonance occurs:

$$\sigma-\omega+\frac{\partial\varphi}{\partial t}\bigg|_{t_0}=0. \tag{41}$$

One then finds

$$S(Z,\sigma)=\frac{\pi}{2}\,\frac{\mathcal{E}^2(t_0)}{|\ddot{\varphi}(t_0)|}, \tag{42}$$

the dots denoting time differentiation. Note that t_0 will, in general, depend on both Z and σ. Equation (42) is valid except in the vicinity of the inflection point defined by $\ddot{\varphi}(t_0)=0$. Then the method of stationary phase is inapplicable. Approximate expressions for the integral in Eq. (40) may then be developed in terms of Airy functions, but we do not pursue them further here. The spectrum may be expressed in terms of derivatives of the phase by using the relation

$$\frac{\partial\varphi}{\partial\eta}=\beta\mathcal{E}^2, \tag{43}$$

which is a restatement of Eq. (9). Then we find

$$S(Z,\sigma)=\frac{\pi}{2\beta}\,\frac{\partial\varphi/\partial\eta}{|(\partial^2\varphi/\partial\xi^2)+2(\partial^2\varphi/\partial\xi\,\partial\eta)+(\partial^2\varphi/\partial\eta^2)|}\bigg|_{t_0}, \tag{44}$$

where t_0 is the root to the equation

$$\sigma-\omega+\frac{\partial\varphi}{\partial\xi}+\frac{\partial\varphi}{\partial\eta}\bigg|_{t_0}=0. \tag{45}$$

In the preresonance domain (e.g., $z<|z_0|$, in the special case considered earlier) Eqs. (45) and (21) imply that t_0 is the root to the following equation:

$$\sigma-\omega+\frac{2z\beta}{v}I'\left(t_0-\frac{z}{v}\right)=0, \tag{46}$$

the prime denoting differentiation with respect to argument. The spectrum may then be expressed as

$$S(Z,\sigma)=\frac{\pi v}{4\beta z}\,\frac{I}{|I''|}\bigg|_{\xi=t_0-z/v}. \tag{47}$$

It should be noted that for $\sigma=\omega_a$ Eqs. (24) and (45) become identical. Thus the line $t=t_0$ and the resonance curve (such as is illustrated in Fig. 7) become one and the same. For $\sigma<\omega_a$ the line $t=t_0$ lies in the preresonance domain (i.e., the domain continguous with $z=0$) so obviously Eq. (47) is valid for $\sigma<\omega_a$. In the case where $\sigma>\omega_a$ the line resides in the postresonance domain and a new expression for $S(Z,\sigma)$ must be sought.

Insertion of Eq. (29) into Eq. (44) yields a formal expression for the spectrum:

$$S(Z,\sigma)=\frac{\pi}{2\beta}\,\frac{G(\xi)}{|F''+\eta G''+2G'|}\bigg|_{t=t_0}. \tag{48}$$

Now t_0 is defined as the root of the equation

$$\sigma-\omega+F'(\xi)+\eta G'(\xi)+G(\xi)|_{t=t_0}=0. \tag{49}$$

Combining these expression with Eq. (30) yields the spectrum

$$S(Z,\sigma)=\frac{\pi}{2\beta}\,\frac{G(\xi)}{|(1-B')G'+(\eta-B)G''|}\bigg|_{t_0}, \tag{50}$$

where t_0 is the root of the equation

$$\eta=B+\frac{\omega_a-\sigma}{G'}. \tag{51}$$

Let us study the particular case of the strong-

absorption limit ($\alpha \to \infty$). Equation (50) is not of particular use here unless we have an explicit solution for $G(\xi)$. However, it is possible to obtain information from Eq. (40) directly through the use of the Schwartz inequality. We have

$$S = \frac{1}{4}\left| \int_{-\infty}^{\infty} dt\, e^{i(\sigma t - \omega t + \varphi)} \frac{\mathcal{E}}{f_0} f_0 \right|^2, \tag{52}$$

where f_0 will be specified shortly. Then

$$S \leq \frac{1}{4}\left(\int_{-\infty}^{\infty} dt\, f_0^2 \right)\left[\int_{-\infty}^{\infty} dt \left(\frac{\mathcal{E}}{f_0}\right)^2 \right]. \tag{53}$$

Use the fact that $\mathcal{E}^2 = G/\beta$ and note that Eq. (35) implies an upper bound on $G(\xi)$,

$$G(\xi) \leq \beta I(\xi)\, e^{-\alpha/2|\beta I'(\xi)|}, \tag{54}$$

to obtain

$$S(Z,\sigma) \leq \frac{1}{4}\left(\int_{-\infty}^{\infty} dt\, f_0^2 \right)\left(\int_{-\infty}^{\infty} dt\, \frac{I}{f_0^2}\, e^{-\alpha/2|\beta I'|} \right). \tag{55}$$

First we note that for pulses the quantity $I'(\xi)$ will attain a maximum. Secondly we choose $f_0^2 = [I(\xi)]^{1/2}$ and note that this is an integrable quantity since $I(\xi)$ describes a pulse (remember, by definition, $I \geq 0$). Thus

$$S(Z,\sigma) \leq \frac{1}{4}\left\{ \int_{-\infty}^{\infty} dt\, [I(\xi)]^{1/2} \right\}^2 e^{-\alpha/2|\beta I'|_{\max}}. \tag{56}$$

The right-hand side vanishes as $\alpha \to \infty$. Thus we arrive at the important result that the spectrum is highly suppressed for frequencies beyond ω_a in the strong-absorption limit!

V. DISCUSSION

In the experimental results it has been noticed that a discontinuity in intensity occurs when the self-phase-modulation frequency extends beyond the absorption-line frequency. This discontinuity is predicted by Eq. (56), which puts an upper limit on the magnitude of the step. In order to obtain an estimate for the theoretical magnitude of the discontinuity one must assign numerical values to the various parameters that have appeared in the theory.

First one must have information concerning the parameters f, γ, and ω_a appearing in Eq. (5). Decay rates and resonant frequencies for excited states of Pr^{3+} have been reported in the literature.[15] The $^1D_2$-to-ground-state transition has a frequency lying to the red side of 5300 Å and the $^3P_{2,1,0}$-to-ground-state transitions lie on the blue side. Let us concentrate on the $^1D_2$ state for the sake of definiteness. Then one has[15] $\gamma = 1.1\times10^3$ sec^{-1} for the radiative lifetime. The quantity f can be determined from a knowledge of the absorption coefficient, and this is discussed in Appendix B. We take $\omega = 3.6\times10^{15}$ rad/sec and replace[17] ϵ_0 by 1 to obtain an approximate estimate. A measurement was made and it was found that for $z = 1$ cm I_f/I_i is roughly 0.1. The laser frequency spread was roughly 10^{11} rad/sec.

Insertion of these parameters into Eq. (B4) yields an estimate for f equal to 10^4 sec^{-1}. Insertion of this into Eq. (16) gives us a value for the parameter α equal to 7×10^{29} sec^{-2}. Unfortunately, a definite value for ϵ_2 for this material is not known to us but one might have, typically, $\epsilon_2/\epsilon_0 \simeq 10^{-12}$ esu. This would define the parameter β appearing in Eq. (17) as $\beta = 700$.

If the input intensity is 8×10^8 W, the pulse duration is 4×10^{-12} sec, the number of self-focused filaments is 50, and the filament diameter is 30 μ. Then the average field strength is $\mathcal{E} = 1.4\times10^5$ esu. One can therefore estimate $I'_{\max}$, appearing in Eq. (56) as $I' \approx \mathcal{E}^2/\tau = 5\times10^{21}$. Then the ratio appearing in the exponent of Eq. (56) becomes

$$\frac{\alpha}{2|\beta I'|_{\max}} = 10^5. \tag{57}$$

This implies an almost total suppression of the signal beyond the absorption resonance. A similar argument and conclusion occurs for the blue side of the laser line. The residual weak intensity that exists beyond the absorption line is not due to self-phase-modulation. It can arise, however, from three-wave mixing (four-photon parametric process).[6,11,18] The previous theory has neglected the study of this phenomenon, but it is known to occur in many systems.[6,11] Since we have a continuum of frequencies created by self-phase-modulation it might be possible for three such frequencies, ω_1, ω_2, and ω_3, to mix to create a signal at frequency $\omega_1 + \omega_2 - \omega_3$ which lies beyond the absorption line. Since the frequencies are chosen from a continuum it is possible for phase matching to be achieved also.

Let us now study the spectrum in the domain lying between the laser frequency and the absorption line. It is convenient now to refer to a Gaussian pulse, such as

$$I = I_0 e^{-\xi^2/\tau^2}. \tag{58}$$

Insertion into Eq. (47) yields the result

$$S(Z,\sigma) = \frac{\pi v}{4\beta z}\left| \frac{1}{(2/\tau^2) - (4/\tau^4)[t_0 - (z/v)]^2} \right|, \tag{59}$$

where $t_0 - (z/v)$ is given by Eq. (46); i.e., one must solve the following transcendental equation:

$$\sigma - \omega - \frac{4z\beta}{v\tau^2} I_0\left(t_0 - \frac{z}{v}\right) \exp -\left(\frac{t_0 - z/v}{\tau}\right)^2 = 0. \tag{60}$$

It is particularly interesting to examine this in the limit where σ is close to ω, so

$$t_0 - \frac{z}{v} \simeq \frac{(\sigma-\omega)v\tau^2}{4z\beta I_0} . \tag{61}$$

If I_0 is sufficiently large this will be small compared to τ and Eq. (59) will reduce to

$$S(Z,\sigma) \simeq \frac{\pi v\tau^2}{8\beta z} , \tag{62}$$

a result independent of I_0. Thus the low-frequency-shifted part of the self-modulated signal is independent of intensity.

To understand the meaning of this it is important to examine the frequency extent of the self-phase-modulation. As one increases the value of σ in Eq. (60) one ultimately reaches a point where no solution to the equation exists any more. It occurs at

$$\sigma - \omega = \frac{4z\beta I_0}{v\tau(2e)^{1/2}} . \tag{63}$$

Thus the extent of the self-broadening is proportional to the intensity. Since the energy in the pulse is proportional to the product of the frequency extent and the intensity spectrum one can now see why the intensity spectrum must remain approximately constant.

It is not a simple matter to detect this constancy, because of the fact that the light tends to break up into self-focused filaments, all of which have roughly the critical power in them. Increasing the incident intensity only creates additional filaments. It is interesting to note that the same parameters determining self-focusing appear in the theory of self-phase-modulation, pointing to a unity in the theory of nonlinear optics.

The observed absorption band in the continuum on the anti-Stokes side at about 400 cm^{-1} away from the excitation frequency (see Fig. 2) is probably due to the inverse Raman effect.[19] The observed absorption band is located in the vicinity where strong Raman bands[16] are found: 401, 370, and 321 cm^{-1}. The inverse Raman spectrum has been observed before in the self-phase-modulated continuum generated in benzene and carbon disulfide.[20]

Finally we point out that if one were actually to compute the intensity of the spectrum given by Eq. (62) the right value of τ should be used. There is evidence[21] that the picosecond pulse actually consists of an envelope of subpicosecond pulses lasting on the order of 2×10^{-13} sec. If this is the case then this value should be employed for τ. As we mentioned earlier, there is evidence in this experiment for superbroadband four-photon collinear and angular parametric generation.[22] A curious feature of the associated weak-broadband spectrum is the existence of a pronounced absorption line at a position (6112 Å) where the linear absorption would be expected to be rather weak.

A possible explanation for this consistent with the previous theory is as follows: Imagine tracing the spatial development of the phase-modulation spectrum. At short distances, where the bounds of the spectrum have not yet intersected a strong absorption line, the spectrum is reasonably flat. Upon intersection with the absorption line we have shown (see Fig. 7) that the spectrum abruptly drops. The mechanism of four-photon parametric generation is presumably responsible for the appearance of the signal beyond the absorption-line limit. Also, this explanation is supported by the appearance of the angular emission pattern (see Fig. 6). As the spectrum continues to develop one reaches a point where the limit of the regenerated spectrum crosses a weak absorption line. The problem is identical with the previously considered theory. One can again expect a drastic drop in the spectrum at the position of this line. At still further distances renewed four-photon parametric regeneration accounts for the feeble signal.

APPENDIX A

In this appendix we work out in some detail the time integration of Eq. (5). The basic integral we are confronted with, after having discarded the antiresonant term, is

$$I = \int_{-\infty}^{0} d\tau\, \mathcal{E}(t+\tau)\, e^{\gamma\tau} \sin[kz - \omega t + (\omega_a - \omega)\tau + \varphi(t+\tau)] . \tag{A1}$$

Two cases can be discussed, depending on the relative size of $1/\gamma$ and the duration of the pulse. Both limits will be examined in this appendix.

If one assumes that the duration of the pulse is long compared with the radiative lifetime, then the factor $e^{\gamma\tau}$ acts to suppress large contributions to the integral, so one has approximately

$$I \approx \int_{-\infty}^{0} d\tau\, \mathcal{E}(t)\, e^{\gamma\tau} \sin[kz - \omega t + (\omega_a - \omega)\tau + \varphi(t) + \dot{\varphi}(t)\tau] , \tag{A2}$$

and the results of Eqs. (7a) and (7b) follow directly. Then a Lorentzian function [see Eq. (10)] appears in the theory.

On the other hand, if the duration of the pulse is short compared with the radiative lifetime, one may neglect γ altogether and obtain

$$I \approx \mathrm{Im} \int_{-\infty}^{0} d\tau\, \mathcal{E}(t+\tau) \exp\{i[kz - \omega t + (\omega_a - \omega)\tau + \varphi(t+\tau)]\} . \tag{A3}$$

It is important to recall that the electric field pulse depends on space also, i.e., $\mathcal{E}(t)=F[t-(z/v)]$, where F is a function peaked at the point $t=z/v$. Our main region of interest lies in the neighborhood of $t=z/v$, so we can write, approximately,

$$\mathcal{E}(t+\tau)=F\left(t-\frac{z}{v}+\tau\right)$$
$$\approx F\left(t-\frac{z}{v}\right)e^{-\lambda\tau^2}. \tag{A4}$$

Here λ describes the curvature of the pulse and is given approximately by $\lambda=(1/D)^2$, D being the pulse duration. Thus Eq. (A3) becomes

$$I\approx \mathrm{Im}\mathcal{E}(t)\exp[i(kz-\omega t)]\int_{-\infty}^{0}d\tau$$
$$\times\exp\{-\lambda\tau^2+i[(\omega_a-\omega)\tau+\varphi(t+\tau)]\}. \tag{A5}$$

Upon linearizing the phase φ (assuming again $\ddot{\varphi}$ is small) one obtains

$$I\simeq \mathrm{Im}\mathcal{E}(t)\exp\{i[kz-\omega t+\varphi(t)]\}\int_{-\infty}^{0}d\tau$$
$$\times\exp\{-\lambda\tau^2+i[\omega_a-\omega+\dot{\varphi}(t)]\tau\}. \tag{A6}$$

A convenient expression is obtained by employing the method of stationary phase to evaluate this integral rather than expressing it exactly in terms of complex error functions. Thus

$$I=\mathcal{E}(t)\sin[kz-\omega t+\varphi(t)]\left(\frac{\pi}{\lambda}\right)^{1/2}$$
$$\times\exp\left(\frac{-[\omega_a-\omega+\dot{\varphi}(t)]^2}{4\lambda}\right). \tag{A7}$$

The important thing to note is that for small λ this reduces to

$$I=\mathcal{E}(t)\sin[kz-\omega t+\varphi(t)]\,2\pi\delta[\omega_a-\omega+\dot{\varphi}(t)]. \tag{A8}$$

Thus, comparing Eq. (A7) with (7a) and (7b) we see that the only difference is the replacement of a Lorentzian representation of the Dirac δ function by a Gaussian representation.

APPENDIX B

In this appendix we relate the strength of the absorption f to the measured absorption parameters. Let us Fourier transform Eq. (5) and assume that the intensity is now weak enough so that the nonlinear term may be discarded. Then we find $D(\omega)=\epsilon(\omega)E(\omega)$, where

$$\epsilon(\omega)=\epsilon_0-\frac{f}{\omega_a-\omega+i\gamma/2}, \tag{B1}$$

and we have dropped the antiresonant term. Using the relation $k=(\omega/c)[\epsilon(\omega)]^{1/2}$ and defining the attenuation constant as $a_{\mathrm{att}}=2\,\mathrm{Im}k$ one has

$$a_{\mathrm{att}}=\frac{2\omega(\epsilon_0)^{1/2}}{c}\,\frac{\gamma f}{4\epsilon_0}\,\frac{1}{(\omega_a-\omega)^2+\frac{1}{4}\gamma^2}$$
$$=a_{\mathrm{att}}(\omega_a-\omega). \tag{B2}$$

The frequency spread of the laser σ_L is here much larger than the decay rate γ. Consequently, as the light propagates through the medium, a hole will be burnt in the frequency profile of the laser. Let $\Delta\omega$ be the extent of this hole and let z be the propagation distance through the crystal. Then the size of the hole will be determined, in terms of order of magnitude, by the condition $a_{\mathrm{att}}(\Delta\omega)z\sim 1$. The ratio $\Delta\omega/\sigma_L$ determines the fraction of power absorbed by the medium and is thus related to the incident and outgoing intensities I_i and I_f, by

$$\frac{\Delta\omega}{\sigma_L}=\frac{I_i-I_f}{I_i}. \tag{B3}$$

Combining Eqs. (B2) and (B3) we finally obtain the desired approximate expression for f:

$$f=\frac{2c(\epsilon_0)^{1/2}\sigma_L^2}{z\omega\gamma}\left(\frac{I_i-I_f}{I_i}\right)^2. \tag{B4}$$

*Research supported in part by Cottrell Research Grant, City University Faculty Award Program and Air Force Office of Scientific Research under Grant No. 71-1978.

†Permanent address: Department of Physics, City College of the City University of New York.

[1]J. Kerr. Phil. Mag. 50, 337 (1875).
[2]W. Voigt, *Magneto and Elektro-Optik* (B. G. Teubner, Leipzig, 1908).
[3]V. S. Starunov, Opt. Spect. (USSR) 18, 165 (1965).
[4]A. Piekara and S. Kielich, Acta Phys. Polon. XVII, 209 (1958); Acta Phys. Polon. XVII, 439 (1958).
[5]S. Kielich, Acta Phys. Polon. 30, 683 (1966); J. Chem. Phys. 46, 4090 (1967); R. Hellwarth, Phys. Rev. 152, 156 (1966).
[6]S. A. Akhmanov, R. V. Khokhlov, and A. P. Sukhorukov, in *Laser Handbook*, Vol. 2, edited by F. T. Arecchi and E. O. Schultz-DuBois (North-Holland, Amsterdam, 1972), Chap. 13.
[7]R. G. Brewer, Phys. Rev. Lett. 19, 8 (1967).
[8]F. Shimizu, Phys. Rev. Lett. 19, 1097 (1967).
[9]R. Polloni, C. A. Sacchi, and O. Svelto, Phys. Rev. Lett. 23, 690 (1969).
[10]R. G. Brewer and C. H. Lee, Phys. Rev. Lett. 21, 267 (1968).
[11]R. R. Alfano and S. L. Shapiro, Phys. Rev. Lett. 24, 584 (1970); Phys. Rev. Lett. 24, 592 (1970); Phys. Rev. Lett. 24, 1217 (1970); Phys. Rev. A 6, 433 (1972).
[12]N. Bloembergen, Optics. Commun. 8, 285 (1973).

[13]B. P. Stoicheff, Phys. Lett. 7, 186 (1963); A. C. Cheung, D. M. Rank, R. Y. Chiao, and C. H. Townes, Phys. Rev. Lett. 20, 786 (1962); M. M. Denariez and J. P. E. Taran, Appl. Phys. Lett. 14, 205 (1969); J. Reintjes, R. L. Carman, and F. Shimizu, Phys. Rev. A 18, 1486 (1973).

[14]N. Bloembergen and P. Lallemand, Phys. Rev. Lett. 16, 81 (1966); T. K. Gustafson, J. Taran, H. Haus, J. R. Lifsitz, and P. L. Kelley, Phys. Rev. 177, 306 (1969); R. Polloni, C. A. Sacchi, and O. Svelto, Phys. Rev. A 2, 1955 (1970); R. A. Fisher, P. L. Kelley, and T. K. Gustafson, Appl. Phys. Lett. 14, 140 (1969); M. M. Denariez Roberge and J. P. E. Taran, Appl. Phys. Lett. 14, 205 (1969).

[15]M. J. Weber, J. Chem. Phys. 48, 4774 (1968); G. H. Dieke and H. M. Crosswhile, Appl. Optics, 2, 675 (1963).

[16]R. P. Bauman and S. P. S. Porto, Phys. Rev. 161, 842 (1967).

[17]The precise value for ϵ_0 is not known.

[18]A. Yariv and J. E. Paerson, in *Progress in Optics*, edited by J. A. Sanders and K. W. H. Stevens (Pergamon, New York, 1969), Vol. 1.

[19]W. J. Jones and B. P. Stoicheff, Phys. Rev. Lett. 13, 657 (1964); R. A. McLaren and B. P. Stoicheff, Appl. Phys. Lett. 16, 140 (1970).

[20]R. R. Alfano and S. L. Shapiro, Chem. Phys. Lett. 8, 631 (1971).

[21]S. L. Shapiro and M. A. Duguay, Phys. Lett. A 28, 698 (1969). M. A. Duguay, J. W. Hansen, and S. L. Shapiro, IEEE J. Quant. Elec. (1969); IEEE J. Quant. Elec. 6, 725 (1970). D. Von der Linde, IEEE J. Quant. Elec. 8, 328 (1972). M. C. Richardson, IEEE J. Quant. Elec. 9, 768 (1973). D. J. Bradley and W. Sibbett, Opt. Commun. 9, 17 (1973).

[22]Calculation of the spectral pattern is not possible because the refractive index of PrF_3 at various wavelengths is unknown and the three-photon parametric up-and-down conversion would complicate the analysis. The similarity between the observed angular pattern in PrF_3 and glass (Ref. 11) strongly suggests that the four-photon process dominates the PrF_3 spectrum.

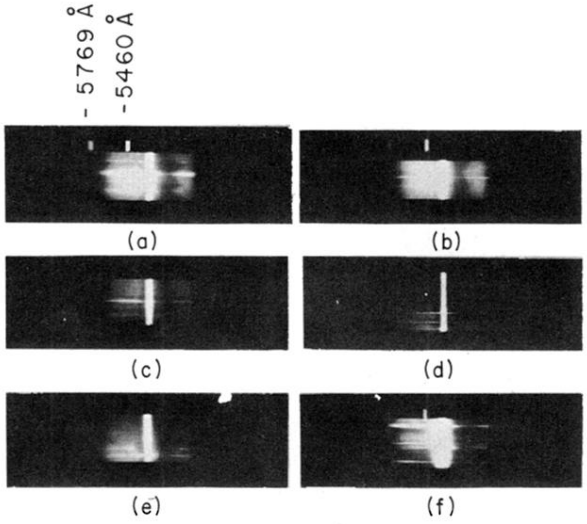

FIG. 2. Frequency broadening from PrF_3 about the 5300-Å psec laser excitation; neutral density (ND) filters: (a) ND = 1.5; (b) ND = 1.5; (c) ND = 2.0; (d) ND = 2.0; (e) ND = 1.7, (f) ND = 1.4. A wire is positioned after the collection lens at the focal length.

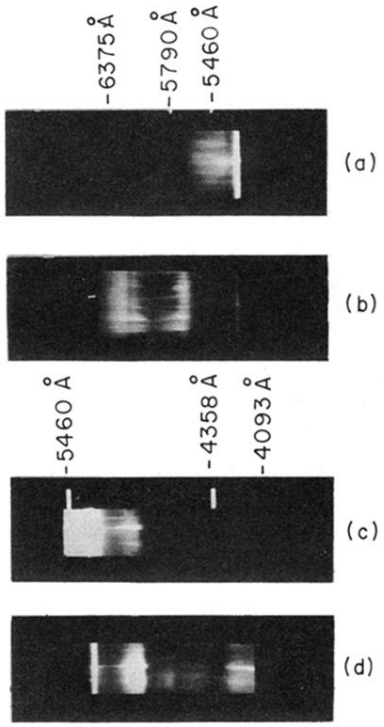

FIG. 3. Frequency broadening on the Stokes and anti-Stokes side of the 5300-Å excitation. (a) Stokes side, Corning 3-68 filter, wire inserted, ND=2.0; (b) Stokes side, Corning 3-66 filter, wire inserted; (c) anti-Stokes side, wire inserted, ND=1.0; (d) anti-Stokes side, Corning 5-61 filter, wire inserted.

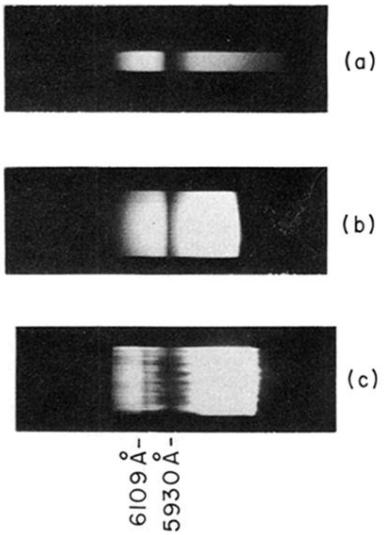

FIG. 4. Comparison of the Stokes absorption spectra of PrF_3 photograph with different light sources: (a) light emitted from a tungsten lamp is passed through 0.5-mm-thick PrF_3 crystal; (b) SPM light emitted from BK-7 is passed through 0.5-mm-thick crystal; (c) SPM light is generated within the 5-cm PrF_3.

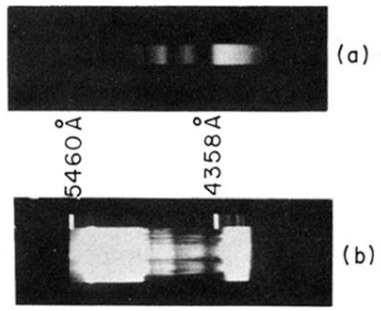

FIG. 5. Comparison of the anti-Stokes absorption spectrum of PrF_3 photograph with (a) light emitted from a tungsten lamp passing through 0.5-mm-thick crystal; (b) SPM light generated within the 5-cm PrF_3.

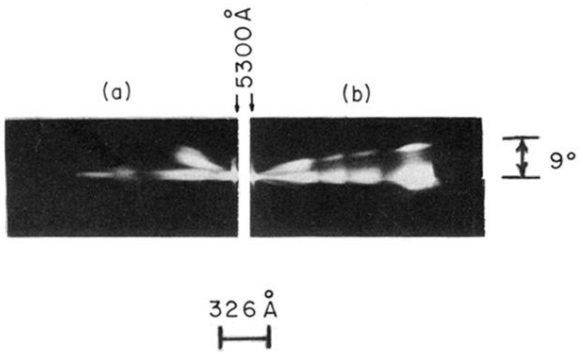

FIG. 6. Angular variation of the (a) Stokes and (b) anti-Stokes spectral patterns emitted from PrF_3 crystal: (a) Corning 4-(3-67) filters, ND = 1.0; (b) Corning 2-(5-60) filters.